

Data-Efficient Sleep Staging with Synthetic Time Series Pretraining

Niklas Grieger^{1,2,3}, Siamak Mehrkanoon², and Stephan Bialonski^{1,3,*}

¹Department of Medical Engineering and Technomathematics, FH Aachen University of Applied Sciences, 52428 Jülich, Germany

²Department of Information and Computing Sciences, Utrecht University, Utrecht, The Netherlands

³Institute for Data-Driven Technologies, FH Aachen University of Applied Sciences, 52428 Jülich, Germany

*bialonski@fh-aachen.de

ABSTRACT

Analyzing electroencephalographic (EEG) time series can be challenging, especially with deep neural networks, due to the large variability among human subjects and often small datasets. To address these challenges, various strategies, such as self-supervised learning, have been suggested, but they typically rely on extensive empirical datasets. Inspired by recent advances in computer vision, we propose a pretraining task termed “frequency pretraining” to pretrain a neural network for sleep staging by predicting the frequency content of randomly generated synthetic time series. Our experiments demonstrate that our method surpasses fully supervised learning in scenarios with limited data and few subjects, and matches its performance in regimes with many subjects. Furthermore, our results underline the relevance of frequency information for sleep stage scoring, while also demonstrating that deep neural networks utilize information beyond frequencies to enhance sleep staging performance, which is consistent with previous research. We anticipate that our approach will be advantageous across a broad spectrum of applications where EEG data is limited or derived from a small number of subjects, including the domain of brain-computer interfaces.

Introduction

Deep neural networks have achieved significant advances in analyzing electroencephalographic (EEG) time series¹, ranging from brain-computer interfaces² to the intricacies of sleep stage scoring^{3,4}. Such successes are attributed to the ability of deep neural networks, as universal function approximators, to learn properties (features) from patient data that are difficult for humans to conceptualize and define. However, training neural networks requires large and diverse datasets that capture the considerable variety between individual subjects and their medical conditions (subject heterogeneity). Creating such datasets is challenging due to the typically limited amount of data per subject (data scarcity) and diverse measurement protocols used in different clinics, which can introduce additional variability in the data. Furthermore, acquiring large datasets is often expensive, complicated, or even intractable due to strict privacy policies and ethical guidelines. This hinders the advancement of deep neural networks for widespread application in real-world medical settings.

Efforts to mitigate the scarcity of large datasets have primarily followed two paths: (1) the development of network architectures that incorporate constraints mirroring the data’s intrinsic characteristics, such as symmetries⁵, and (2) enhancing model performance through the use of additional or cross-domain data to learn effective priors. Pertaining to the first path, a common feature in time series processing networks is the use of convolutional layers. These layers are designed to be translation-equivariant⁶, which ensures that a temporal shift in the input only affects the output by the same shift. This characteristic enables consistent network responses to temporal patterns, regardless of their temporal location, while reducing the number of model parameters compared to architectures lacking such constraints. For the second path, a variety of strategies have been proposed to learn useful priors from data. One approach is data augmentation, in which time series are transformed while preserving their annotations (labels) to artificially expand the dataset^{7,8}. Deep neural networks trained on such augmented datasets implicitly learn to become invariant under these transformations, which can lead to better out-of-sample prediction performance. Another strategy is transfer learning⁹, a two-step process in which neural networks are trained on one task using a large dataset (pretraining step¹⁰) and then adapted to learn the actual task of interest using another (usually much smaller) dataset (fine-tuning step). A variant of this idea is self-supervised learning^{11,12}, which allows neural networks to be pretrained on large and heterogeneous datasets without explicitly labeled examples. Finally, generative models such as GANs can be used to sample new time series to extend existing datasets^{13,14}. Such generative models approximate a data distribution and require large heterogeneous datasets for training. While all of these approaches have been demonstrated to be able to improve the

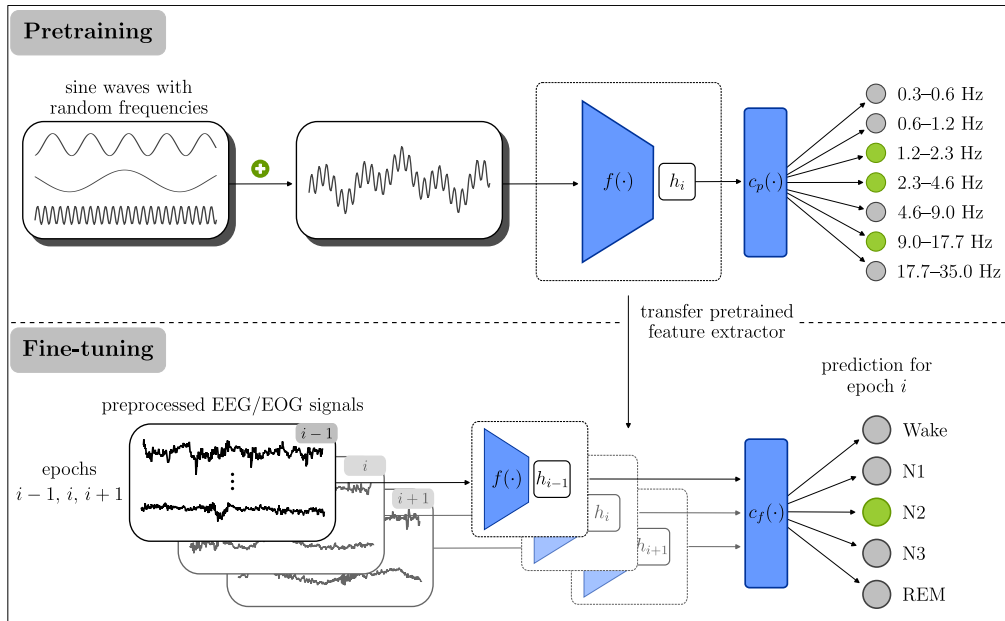


Figure 1. The training process consists of a *pretraining* and a *fine-tuning* phase. In the pretraining phase, the feature extractor f produces features h_i and is trained together with a classifier c_p to detect the frequency content of randomly generated synthetic time series signals (multi-label classification problem). In the fine-tuning phase, the pretrained feature extractor f extracts features h_i from individual epochs of EEG and EOG signals. The features of a sequence of epochs (training sample) are then aggregated by a classifier c_f to predict the sleep stage of the middle epoch in the sequence (multi-class classification problem).

performance of neural networks, they still rely on large empirical datasets for training.

Recent advances in computer vision have demonstrated that it is possible to learn effective priors exclusively from synthetic images, which has the potential to significantly reduce the need for large empirical datasets^{15,16}. Synthetic images for image classification tasks were generated by simple random processes, such as iterated function systems to produce fractals¹⁶ or random placement of geometric objects to cover an image canvas¹⁵. Deep neural networks pretrained on such data were demonstrated to learn useful priors for image classification tasks, yielding competitive performance comparable to pretraining on natural images on various benchmarks¹⁶. This remarkable finding highlights the potential of synthetic datasets that can be generated without much computational resources and, theoretically, in unlimited amounts.

Inspired by these advances, we hypothesize that pretraining exclusively on synthetic time series data generated from simple random processes can also yield effective priors for sleep staging. Given the importance of frequencies for sleep stage scoring and other EEG-based applications^{17,18}, we introduce a pretraining method that centers on generating synthetic time series data with specific frequency content (see Fig. 1). During pretraining, deep neural networks learn to accurately predict the frequencies present in these synthetic time series. We observe that this conceptually simple pretraining task, which we call “frequency pretraining” (FPT), allows a deep neural network to detect sleep stages with better accuracy compared to fully supervised training when few samples (few-samples regime) or data from few subjects (few-subject regime) are available for fine-tuning (see Fig. 2). The success of our method underscores the essential role of frequency content in enabling neural networks to accurately and reliably discern sleep stages. We consider pretraining techniques leveraging synthetic data, like the one we propose, as a promising area of research, offering the potential to develop models in sleep medicine and neuroscience that are particularly suited for scenarios involving small datasets. To facilitate testing and further advancements, we make the source code of our method publicly available¹⁹.

Methods

Fig. 1 presents an overview of our training scheme, which comprised two phases. In the *pretraining phase*, we generated synthetic time series signals and trained a convolutional feature extractor with a multi-layer perceptron classifier to predict the frequency content of these signals. In the *fine-tuning phase*, we utilized the pretrained feature extractor together with another classifier to perform sleep staging on EEG and EOG (electrooculography) signals.

Data

Synthetic Data

For the pretraining phase (see Fig. 1), we defined a simple random process to generate synthetic time series signals. Each synthetic signal $s_c(t)$ was a normalized time series composed of the sum of 30-second sine waves sampled at 100 Hz with random frequencies and phases,

$$s_c(t) = \frac{\tilde{s}_c(t) - \mu_c}{\sigma_c}, \quad \tilde{s}_c(t) = \sum_i^{n_f} I_i \sin(2\pi f_{c,i} t + \phi_i), \quad I_i \in \mathcal{U}\{0, 1\} \quad (1)$$

where t denotes time (in seconds), n_f denotes the number of frequency bins, I_i denote whether a frequency bin is used (1) or not (0), $f_{c,i}$ denote the frequencies of the sine waves (in Hertz), ϕ_i denote their phase (in radians), and μ_c and σ_c denote mean and standard deviation of \tilde{s}_c . The phases ϕ_i of the sine waves were sampled from a uniform distribution between 0 and 2π . To sample the frequencies $f_{c,i}$, we first divided the frequency range of 0.3–35 Hz recommended by the American Academy of Sleep Medicine (AASM) for filtering EEG and EOG signals into $n_f = 20$ bins with a base 2 logarithmic scale (see x-axis of Fig. 4c for the resulting frequency bins). We chose a logarithmic scale for the frequency bins because typical power spectral densities of EEG and EOG signals show more power in lower frequency bands than in higher bands. We then randomly decided for each frequency bin (with a probability of 50% for each bin) whether it would be used to create the synthetic signal ($I_i = 1$) or not ($I_i = 0$). Within each selected frequency bin, we randomly sampled the final frequencies $f_{c,i}$ of the sine waves. Finally, the generated sine waves were summed and normalized to create synthetic signals $s_c(t)$.

When pretraining our neural networks, each training sample $s(t) = (s_1(t), s_2(t), s_3(t))$ consisted of three synthetic signals, corresponding to three “channels” of sleep staging data, and an associated label vector $l = (I_0, \dots, I_{n_f})$. The three synthetic signals of a sample shared the same phases and frequency bins. However, the frequencies of the sine waves were sampled independently for each channel. The label vector l encoded the frequency bins from which the frequencies of the sine waves were drawn in a one-hot encoded format. Pretraining involved predicting all frequency bins encoded in this label vector l , which made it a multi-label classification problem with $n_f = 20$ classes. For each training run, we generated 101,000 synthetic samples, using 100,000 samples for training and the remaining 1000 samples for tracking various metrics during training. The number of synthetic samples, frequency bins, and the logarithmic scale that defines the boundaries between the bins were determined through preliminary experiments where we explored different hyperparameters.

Sleep Staging Data

During the fine-tuning phase (see Fig. 1), we used two publicly available datasets: the DODO and DODH datasets²⁰. The DODO dataset contains 55 recordings from subjects diagnosed with obstructive sleep apnea (OSA), while the DODH dataset contains 25 recordings from healthy subjects. Each recording stems from a different subject and was split into 30-second non-overlapping windows (epochs), which were annotated with sleep stages (Wake, N1, N2, N3, REM) by five sleep experts following the AASM guidelines¹⁷. Inspired by the work of Guillot et al.²⁰, we used the annotations of all five scorers to create a consensus annotation for each epoch. To create this consensus, we selected the most voted stage for each epoch. In cases of ties, we chose the sleep stage determined by the most reliable scorer. For each recording, the most reliable scorer was identified as the scorer with the highest average agreement with all other scorers. In our experiments, we focused on the following EEG and EOG derivations that are available in both datasets and follow the AASM recommendations¹⁷: C3_M2, F3_M2, EOG1. All channels were sampled at 250 Hz.

To prepare the data for training, we filtered the signals between 0.3 and 35 Hz with an 8th-order Butterworth filter and downsampled the filtered signals to 100 Hz using polyphase filtering. Next, we removed all epochs from the data that were annotated as artifacts by the consensus of the sleep experts. We then normalized the amplitudes of each individual epoch by subtracting the mean and dividing the result by the interquartile range of its amplitude distribution. Finally, we clipped all signal amplitudes above 20 or below -20 to minimize outliers.

After preprocessing the signals, we combined the DODO and DODH datasets into a single dataset of 80 recordings. We then split the data subject-wise into 5 folds for cross-validation using stratified sampling. Consequently, each fold contained 16 recordings, with 11 recordings from the DODO dataset and 5 recordings from the DODH dataset. In addition to splitting the data into training and test folds, we reserved two recordings from each fold as validation data for hyperparameter tuning and early stopping. We validated our models on the validation data of the four training folds. The validation data of the test fold was kept separate and not involved in validation or testing.

Model

We based our model architecture on the TinySleepNet architecture, a conceptually simple deep neural network for sleep staging that has previously demonstrated competitive results²¹. This architecture consists of a convolutional feature extractor that

extracts features from individual epochs and a classifier that aggregates these feature across multiple epochs to perform sleep staging. Our feature extractor consisted of four convolutional layers with 128 filters each, a kernel size of 50, 8, 8, and 8, respectively, and a stride of 25, 1, 1, and 1, respectively. Following each convolutional layer was a batch normalization layer and a ReLU activation function. The outputs of the first and last convolutional layer were passed through max pooling layers that reduced the temporal dimension of the feature maps by a factor of 8 and 4, respectively. Both max pooling layers were followed by a dropout layer with a dropout rate of 0.5.

The feature extractor was followed by a classifier, which had a different architecture in the pretraining phase than in the fine-tuning phase. During pretraining, the classifier consisted of a dense layer with 80 neurons and ReLU activation function, followed by a dense layer with 20 neurons and sigmoid activation function to predict frequency bins. During fine-tuning, the classifier comprised a bidirectional Long-Short Term Memory (LSTM)²² layer with a hidden size of 128, a dropout layer with dropout rate 0.5, and a dense layer with 5 neurons and softmax activation function to predict sleep stages. The classifier used for fine-tuning is similar to the original TinySleepNet classifier, except that the unidirectional LSTM layer was replaced with a bidirectional LSTM layer²¹.

Pretraining

In the pretraining phase, we generated synthetic time series signals by summing sine waves with random frequencies (see section “[Synthetic Data](#)”), and then trained models to identify the frequency bins from which these frequencies were drawn for a given signal (see Fig. 1). Each frequency bin was represented by a single output neuron of the model, with output values greater than 0.5 indicating that the corresponding frequency bin was used to generate the input signal. We trained the models for 20 training epochs using the Adam optimizer²³, a fixed learning rate of 10^{-4} , a batch size of 64, and a binary cross-entropy loss. This loss function is commonly employed for multi-label classification problems with one-hot encoded labels. It is defined as

$$L_{bce} = -\frac{1}{N} \frac{1}{n_f} \sum_{i=1}^N \sum_{j=1}^{n_f} y_{i,j} \cdot \log(\hat{y}_{i,j}) + (1 - y_{i,j}) \cdot \log(1 - \hat{y}_{i,j}), \quad (2)$$

where N is the number of samples, n_f is the number of frequency bins, $y_{i,j}$ is the true label of sample i for class j , and $\hat{y}_{i,j}$ is the predicted label of sample i for class j .

In addition to the loss function, we recorded the hamming metric on the training and validation data after each training epoch. This metric is derived from the hamming loss, a common metric for multi-label classification problems²⁴. Specifically, the hamming metric tracks the fraction of correctly predicted frequency bins and is defined as

$$H = \frac{1}{N} \frac{1}{n_f} \sum_{i=1}^N \sum_{j=1}^{n_f} I_{\{y_{i,j}=\hat{y}_{i,j}\}}, \quad (3)$$

where I is the indicator function, N is the number of samples, n_f is the number of frequency bins, $y_{i,j}$ is the true label of sample i for class j , and $\hat{y}_{i,j}$ is the predicted label of sample i for class j .

Fine-Tuning

In the fine-tuning phase, we trained models to predict sleep stages based on sequences of sleep staging data (see Fig. 1). Each sequence (training sample) consisted of 11 epochs, and the feature extractor of our model generated features for each individual epoch. The LSTM-based classifier then aggregated these features and predicted the sleep stage of the middle epoch in the input sequence. To ensure that the model could use the same aggregation process for all epochs of a recording, we padded the first and last five sequences of each recording with zeros to the full sequence length.

We fine-tuned the models using the Adam optimizer²³, a fixed learning rate of 10^{-4} , weight decay of 10^{-3} , a batch size of 32, and the categorical cross-entropy loss. To prevent overfitting, we limited each training run to a maximum of 50 training epochs and stopped training early if the loss on the validation data did not improve for 10 training epochs (early stopping). Additionally, we clipped all gradients with a maximum norm greater than 5.0 to prevent exploding gradients.

To track model performance during fine-tuning, we recorded the macro F1 score on the training and validation data after each training epoch. In multi-class settings, the macro F1 score is calculated as the average F1 score²⁵ across all classes and is defined as

$$\overline{F_1} = \frac{1}{k} \sum_{i=1}^k 2 \cdot \frac{p_i \cdot r_i}{p_i + r_i}, \quad (4)$$

where k is the number of classes, p_i is the precision for class i , and r_i is the recall for class i .

Results

Training Configurations

We developed several training configurations to investigate the effectiveness of our pretraining method and the relevance of the learned features for sleep staging. In our experiments, we compared the performance of pretrained models against the performance of non-pretrained models in scenarios with varying amounts of training data. In particular, we studied the performance of our approach in *few-samples* and *few-subject* regimes, where the greatest benefit was expected. Furthermore, we analyzed the *priors* that the model learned during pretraining and the role of frequency information in the learned features. Finally, we investigated whether these features could be further improved by fine-tuning the feature extractor. To answer these questions, we created four training configurations.

Fully Supervised. The Fully Supervised training configuration is similar to many existing deep learning approaches for sleep staging³ and served as a baseline to compare our pretrained models against. In this configuration, we skipped the pretraining step and trained (fine-tuned) the model from scratch using sleep staging data.

Fixed Feature Extractor. We employed the Fixed Feature Extractor configuration to investigate the relevance of the features generated by the pretrained feature extractor for sleep staging. After pretraining the feature extractor, we kept its model weights fixed and only fine-tuned the sleep staging classifier.

Fine-Tuned Feature Extractor. With this training configuration, we studied (i) how model performance changes when the pretrained feature extractor is allowed to change during fine-tuning and (ii) whether the *priors* learned during pretraining can prevent overfitting in *few-samples* or *few-subject* regimes. As in the previous configuration, we first pretrained the feature extractor, but then fine-tuned the full model without keeping any model weights fixed. Consequently, this configuration is similar to the Fully Supervised configuration with the key distinction that the feature extractor is initialized with pretrained weights.

Untrained Feature Extractor. The Untrained Feature Extractor configuration was used as a baseline to study whether our pretraining scheme produces *priors* that are superior to random weights for sleep staging. We randomly initialized the feature extractor using He initialization²⁶ and then kept its weights fixed while fine-tuning the classifier. This approach mirrors the Fixed Feature Extractor configuration, but with a random feature extractor instead of a pretrained one.

In all four training configurations, we performed training using the cross-validation scheme described in section “[Sleep Staging Data](#)”. A single training run in this cross-validation scheme included both pretraining and fine-tuning where applicable. If not specified otherwise, all reported results were obtained on the test folds of the cross-validation splits, while the small part of the training data reserved for validation was used as early stopping set during fine-tuning.

To ensure comparability between different training and data configurations, we seeded the model initialization, the synthetic data generation during pretraining, and the data subsampling when fine-tuning with a limited amount of training data. By using the same seeds for all training configurations, we reduced the influence of random initialization and data sampling on comparisons between training configurations. Furthermore, when training with a reduced amount of data, we maintained a constant number of gradient updates per training epoch by duplicating each training sample $\lfloor \frac{N}{N_{red}} \rfloor$ times, where N is the number of samples in the full training data and N_{red} is the number of samples after reduction.

Data Efficiency

To assess the data efficiency of our pretraining method, we trained models from each of the training configurations with the data of a varying number of subjects. The number of subjects in the training data only affected the fine-tuning step, as the pretraining step utilized the same amount of synthetic data regardless of the training data size. A maximum of 56 subjects was available for training, divided into 4 training folds with 14 training subjects (and 2 validation subjects) each. From this pool, we randomly sampled $n_{subj} \in \{1, 2, 5, 10, 25, 56\}$ subjects to create the training data for a single training run. For each number of subjects n_{subj} , we conducted three repetitions of a 5-fold cross-validation scheme, resulting in 15 training runs with 15 macro F1 scores for each training configuration and number of subjects. This approach allowed us to estimate the spread of the macro F1 scores when using different model initializations and data folds for training and testing. Aggregating the scores of multiple training runs was especially important in situations with very little training data, where model performance varied greatly between runs.

Fig. 2 shows the sleep staging performance of the different training configurations (quantified by macro F1 scores) and how this performance depended on the number of subjects included in the training data. The pretrained feature extractors learned features that are more informative for sleep staging than those generated by a random feature extractor. This is especially evident in the low-data regime, where the performance gap between the untrained feature extractor and fixed feature extractor configurations was largest (delta of 0.22 in the average macro F1 score when trained with the data of one subject). Both configurations benefited from an increasing number of subjects in the training data, but the performance gap between the two

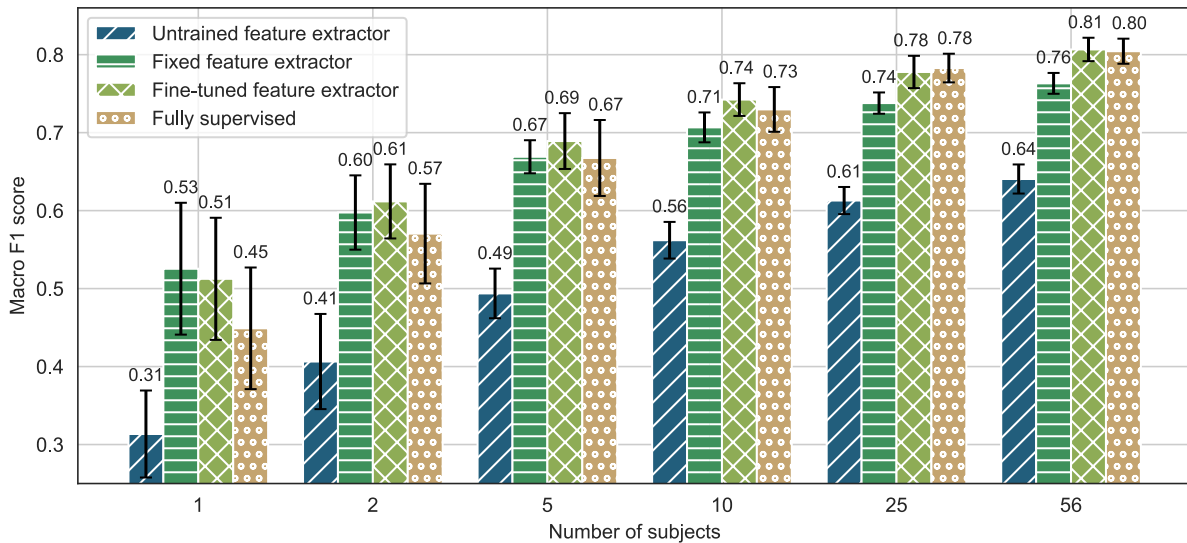


Figure 2. Average macro F1 scores of the different training configurations trained with data from a varying number of subjects. The bars indicate the mean of the macro F1 scores averaged over 15 trainings (3 repetitions of a 5-fold cross-validation) for each training configuration and number of subjects. Error bars show the standard deviation of the macro F1 scores.

configurations remained substantial even when trained with the data of all 56 subjects (delta of 0.12 in the average macro F1 score).

When comparing the fixed feature extractor to the fully supervised configuration, our pretraining scheme again appears to be most beneficial in the low-data regime. The fixed feature extractor configuration outperformed the fully supervised configuration by 0.08 in the average macro F1 score when trained with data from only one subject. This performance gap narrowed as more subjects were included in the training data, until both configurations achieved comparable macro F1 scores of 0.67 when trained with data from five subjects. Training with more than five subjects resulted in the fully supervised configuration outperforming the fixed feature extractor configuration.

Fine-tuning the feature extractor after pretraining appeared to combine the advantages of the fixed feature extractor configuration in the low-data regime and the fully supervised configuration in the high-data regime. When trained with the data of only one subject, the fine-tuned feature extractor configuration achieved an average macro F1 score of 0.51, which was close to the performance of the fixed feature extractor configuration (macro F1 score of 0.53) and outperformed the fully supervised configuration (macro F1 score of 0.45). When fine-tuned with the full training data, the fine-tuned feature extractor configuration achieved an average macro F1 score of 0.81, which was on par with the performance of the fully supervised configuration (macro F1 score of 0.80) and outperformed the fixed feature extractor configuration (macro F1 score of 0.76). Overall, the fine-tuned feature extractor configuration achieved similar or better performance than the other training configurations across all numbers of subjects in the training data.

Few-Samples and Few-Subject Regimes

In the previous experiment, we controlled the amount of data available for training subject-wise, which influenced both (i) the total amount of training samples (moving towards the *few-samples* regime) and (ii) the diversity of the subjects these samples stem from (moving towards the *few-subject* regime). To disentangle the impact of these two factors on model performance, we carried out a second experiment where we controlled the total number of training samples and the diversity of the subjects in the training data separately. We randomly sampled $n_{subj} \in \{1, 2, 3, 4, 5\}$ subjects from the training data and then randomly sampled $n_{samples} \in \{50, 130, 340, 900, all\}$ training samples from the combined data of these subjects (“all” indicates that all available training samples were used). As in the first experiment, we conducted three repetitions of 5-fold cross-validation for each parameter combination. This experiment only focused on the fully supervised and fine-tuned feature extractor training configurations.

Fig. 3 shows the effects that subject diversity and training sample volume had on sleep staging performance. The results demonstrate that both the fully supervised and the fine-tuned feature extractor configurations benefited from an increased subject diversity, even if the total number of training samples was kept constant (see rows in figures 3a and 3b, respectively). Similarly, both configurations benefited from an increased number of training samples when keeping the number of subjects constant (see columns in figures 3a and 3b). Overall, the impact that a reduced subject diversity had on model performance

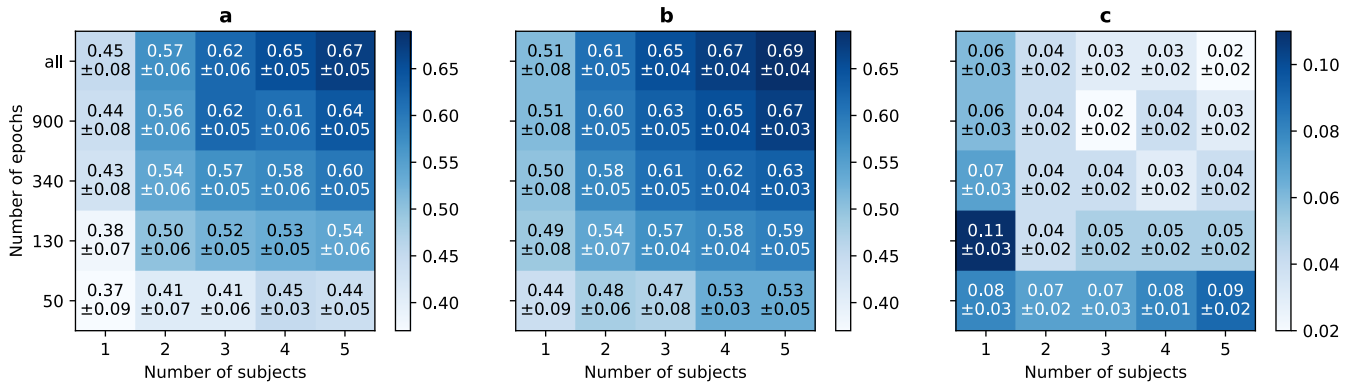


Figure 3. Detailed comparison of the *Fully Supervised* and *Fine-Tuned Feature Extractor* configurations in *few-samples* and *few-subject* regimes. Panels **a** and **b** show the mean and the standard deviation of the macro F1 scores over 15 trainings (3 repetitions of a 5-fold cross-validation) of the fully supervised trained and the fine-tuned feature extractor configurations, respectively. Panel **c** shows the average macro F1 scores achieved by the fine-tuned feature extractor configuration minus the average macro F1 scores achieved by the fully supervised configuration. These differences were calculated using a bootstrapping approach with 10,000 bootstrap samples. For each bootstrap sample, we first sampled 15 macro F1 scores with replacement from the 15 values available for each matrix entry. Then, we calculated the difference between the averages of the sampled scores. Finally, we display the mean and the standard deviation over these bootstrap samples.

appeared to be comparable to the impact of a reduced number of training samples.

Similar to the observations made in section “[Data Efficiency](#)”, the fine-tuned feature extractor configuration generally achieved better macro F1 scores than the fully supervised configuration both in *few-samples* (see lower part of Fig. 3c) and *few-subject* regimes (see left part of Fig. 3c). The pretrained models outperformed the fully supervised models by up to 0.11 in macro F1 score. This highlights the potential of our pretraining scheme in situations where only a few subjects and/or annotated epochs are available.

Priors Towards Frequency Information

To get a better understanding of the pretraining process and the *priors* learned by the model, we recorded several metrics during pretraining. Fig. 4 shows the development of the loss function and the hamming metric during a single pretraining run. Additionally, it shows the accuracy of the fully pretrained model to predict frequencies belonging to each of the 20 frequency bins. The loss function in Fig. 4a converged to a low value, indicating that the model has learned effectively. At the same time, the hamming metric in Fig. 4b reached a high value of 0.9 on the validation data. This value can be interpreted as the model predicting the frequency bins that were used to create the synthetic signals with an accuracy of 90%. Interestingly, Fig. 4c shows that the model was especially proficient in predicting higher frequencies starting from 2.5 Hz (accuracies > 90%). Lower frequencies, especially those below 1 Hz, were predicted with lower accuracy (75–85%).

We hypothesize that the differences in prediction accuracy across frequency bins are not due to the pretrained model being unable to predict lower frequencies. Instead, we believe this discrepancy arises from the varying width of the frequency bins (see x-axis of Fig. 4c). Due to their logarithmic scaling, the bins for lower frequencies were narrower than those for higher frequencies. This could potentially make it more challenging for the model to distinguish between the lower frequency bins.

Discussion

In this work, we propose a novel pretraining scheme for EEG time series data that leverages synthetic data generated by a simple random process. We hypothesize that our pretraining scheme could be particularly beneficial in *few-samples* and *few-subject* regimes, which we argue could benefit greatly from the *priors* towards frequency information that a model learns during pretraining.

Our results confirm the effectiveness of our pretraining scheme, particularly in *few-samples* and *few-subject* regimes. Pretrained models outperformed fully supervised models when trained with a reduced number of subjects or training samples (see columns and row in Fig. 3c, respectively). This supports observations made in the field of Self-Supervised Learning (SSL) that pretrained models generally have better data efficiency than fully supervised ones^{12,27}. In contrast to SSL methods, however, our pretraining scheme improves data efficiency without requiring empirical data. We hypothesize that this effect is caused by the *priors* that the model learns during pretraining. These *priors* could prevent overfitting to a small number of training samples, particularly those from minority classes (e.g., N1), or subject-specific features, which is especially problematic

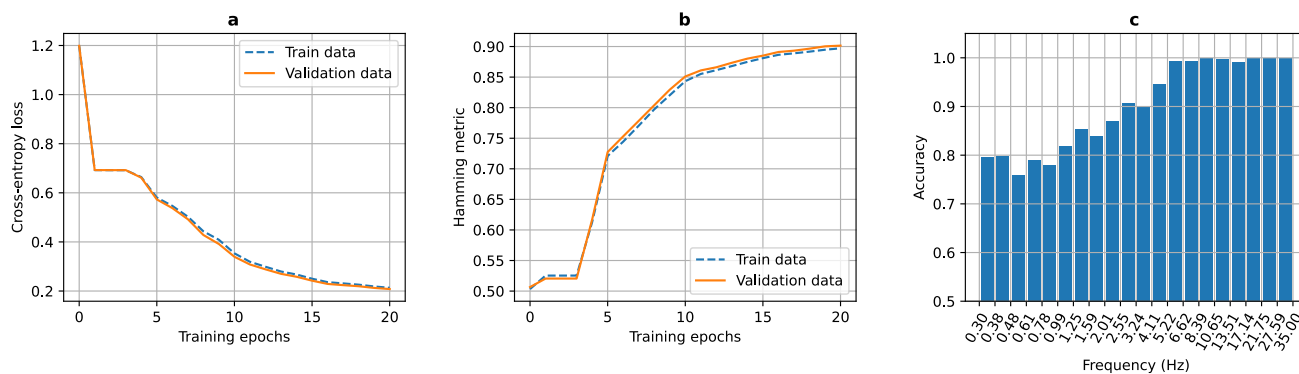


Figure 4. Pretraining metrics of a single pretraining run. Panel **a** shows the development of the loss function during pretraining for both the training and validation data. The following two panels quantify the accuracy of the model to predict the frequencies of the synthetic signals. The hamming metric in panel **b** measures the overall accuracy summarized across all frequency bins, while panel **c** shows the accuracy for each frequency bin separately.

in situations with very little training data. As expected, we observed that all of our training configurations improved with a larger training dataset (see Fig. 2). This aligns with the prevalent view in the literature that deep learning models for sleep staging need substantial amounts of diverse data to perform well^{3,4,28,29}. When trained with the full training data, pretrained models performed comparably to fully supervised models (see Fig. 2), achieving macro F1 scores similar to those of other deep learning approaches for sleep staging^{3,30}.

We further observed that, while the frequency content of a signal is crucial for sleep staging, deep neural networks are capable of extracting additional information from the data that exceeds the frequency domain. The importance of the frequency content of a signal for sleep staging is demonstrated by the high macro F1 scores achieved by the fixed feature extractor configuration and the substantial performance improvements it achieved over untrained feature extractors (see Fig. 2). We attribute the performance gap between the two training configurations to the *priors* learned during pretraining the feature extractor. These *priors* biased the model to extract frequency information from the data, which it achieved with high accuracy after pretraining (see Fig. 4b and c). Our finding is consistent with previous studies that reported frequency-based features to be important for sleep staging¹⁸. When the feature extractor of our model was allowed to be fine-tuned after pretraining, model performance increased in all data regimes (except for the lowest data regime with only one subject; see Fig. 2). We hypothesize that this increase in the macro F1 score is due to the feature extractor learning to extract information beyond the frequency content of the signal during fine-tuning. This hypothesis is in line with the AASM annotation guidelines¹⁷, which consider several frequency-unrelated features essential for sleep staging. These features include time-domain information, which is important for spindles, as well as amplitudes and specific patterns, such as k-Complexes⁴. Recent studies that applied feature engineering approaches to sleep staging further support our hypothesis by including additional features from the time-domain in their models^{31,32}. In one study, the authors analyzed the most important features for their model and found that time-related features, such as the time elapsed from the beginning of a recording, were among the top 20 most important features³¹. Although it remains unclear what additional information our pretrained models learn during fine-tuning, our method offers a promising avenue for future research into the interpretability of deep neural networks for sleep staging.

There are several opportunities for future work that could build upon our findings. One promising direction is to explore the pretraining task in more detail, for example, by investigating the impact of changing the frequency range that is used to generate the synthetic signals during pretraining. Similar to previous work in the vision domain¹⁵, it could also be promising to investigate which structural properties of synthetic time series are important for sleep staging. This could be achieved by defining new pretraining tasks that are based on different data generation processes and may lead to a better understanding of what constitutes “natural” EEG time series. In addition, we suggest exploring models with greater capacity and less inductive bias, such as transformer models^{33,34}, which we expect to benefit even more from our pretraining method. Pretraining such models with synthetic data may alleviate their need for large amounts of training data³⁵. Another avenue for future research is to investigate the generalizability of our method to more diverse datasets. In this work, we tested our method only on two datasets with two different pathologies (healthy and diagnosed with sleep apnea). Initiatives such as the sleepdata.org platform³⁶ and the Temple University data corpus³⁷ provide a wide range of datasets that could be used for this purpose. Finally, it could be insightful to compare our approach with recent SSL methods¹¹ and data augmentation strategies that employ synthetic EEG generators^{7,13}. To enable such comparisons and to facilitate future research in this direction, we make our code available online¹⁹.

Our method presents a novel solution to address important issues that affect current deep learning models in the EEG time series domain, without requiring large amounts of patient data. We expect our approach to be advantageous in various applications where EEG data is scarce or derived from a limited number of subjects, such as brain-computer interfaces².

References

1. Roy, Y. *et al.* Deep learning-based electroencephalography analysis: A systematic review. *J. Neural Eng.* **16**, 051001, DOI: [10.1088/1741-2552/ab260c](https://doi.org/10.1088/1741-2552/ab260c) (2019).
2. Ko, W., Jeon, E., Jeong, S., Phyo, J. & Suk, H.-I. A survey on deep learning-based short/zero-calibration approaches for EEG-based brain–computer interfaces. *Front. Hum. Neurosci.* **15**, DOI: [10.3389/fnhum.2021.643386](https://doi.org/10.3389/fnhum.2021.643386) (2021).
3. Phan, H. & Mikkelsen, K. Automatic sleep staging of EEG signals: Recent development, challenges, and future directions. *Physiol. Meas.* **43**, 04TR01, DOI: [10.1088/1361-6579/ac6049](https://doi.org/10.1088/1361-6579/ac6049) (2022).
4. Fiorillo, L. *et al.* Automated sleep scoring: A review of the latest approaches. *Sleep Med. Rev.* **48**, 101204, DOI: [10.1016/j.smrv.2019.07.007](https://doi.org/10.1016/j.smrv.2019.07.007) (2019).
5. Bronstein, M. M., Bruna, J., Cohen, T. & Velickovic, P. Geometric deep learning: Grids, groups, graphs, geodesics, and gauges. *CoRR* **abs/2104.13478**, DOI: [10.48550/arxiv.2104.13478](https://doi.org/10.48550/arxiv.2104.13478) (2021).
6. Goodfellow, I. J., Bengio, Y. & Courville, A. C. *Deep Learning*. Adaptive computation and machine learning (MIT Press, Cambridge, Massachusetts, 2016).
7. Lashgari, E., Liang, D. & Maoz, U. Data augmentation for deep-learning-based electroencephalography. *J. Neurosci. Meth.* **346**, 108885, DOI: [10.1016/j.jneumeth.2020.108885](https://doi.org/10.1016/j.jneumeth.2020.108885) (2020).
8. He, C., Liu, J., Zhu, Y. & Du, W. Data augmentation for deep neural networks model in EEG classification task: A review. *Front. Hum. Neurosci.* **15**, DOI: [10.3389/fnhum.2021.765525](https://doi.org/10.3389/fnhum.2021.765525) (2021).
9. Ebbelohj, A., Thunbo, M. Ø., Andersen, O. E., Glindtvd, M. V. & Hulman, A. Transfer learning for non-image data in clinical research: A scoping review. *PLOS Digit. Heal.* **1**, e0000014, DOI: [10.1371/journal.pdig.0000014](https://doi.org/10.1371/journal.pdig.0000014) (2022).
10. Qiu, Y., Lin, F., Chen, W. & Xu, M. Pre-training in medical data: A survey. *Mach. Intell. Res.* **20**, 147–179, DOI: [10.1007/s11633-022-1382-8](https://doi.org/10.1007/s11633-022-1382-8) (2023).
11. Liu, Z., Alavi, A., Li, M. & Zhang, X. Self-supervised contrastive learning for medical time series: A systematic review. *Sensors* **23**, DOI: [10.3390/s23094221](https://doi.org/10.3390/s23094221) (2023).
12. Banville, H., Chehab, O., Hyvärinen, A., Engemann, D.-A. & Gramfort, A. Uncovering the structure of clinical EEG signals with self-supervised learning. *J. Neural Eng.* **18**, 046020, DOI: [10.1088/1741-2552/abca18](https://doi.org/10.1088/1741-2552/abca18) (2021).
13. Habashi, A. G., Azab, A. M., Eldawlatly, S. & Aly, G. M. Generative adversarial networks in EEG analysis: An overview. *J. NeuroEng. Rehabil.* **20**, DOI: [10.1186/s12984-023-01169-w](https://doi.org/10.1186/s12984-023-01169-w) (2023).
14. Carrle, F. P., Hollenbenders, Y. & Reichenbach, A. Generation of synthetic EEG data for training algorithms supporting the diagnosis of major depressive disorder. *Front. Neurosci.* **17**, DOI: [10.3389/fnins.2023.1219133](https://doi.org/10.3389/fnins.2023.1219133) (2023).
15. Baradad, M., Wulff, J., Wang, T., Isola, P. & Torralba, A. Learning to see by looking at noise. In Ranzato, M., Beygelzimer, A., Dauphin, Y. N., Liang, P. & Vaughan, J. W. (eds.) *Annu. Conf. on Neural Information Processing Systems, NeurIPS*, 2556–2569 (virtual, 2021).
16. Kataoka, H. *et al.* Pre-training without natural images. *Int. J. Comput. Vis.* **130**, 990–1007, DOI: [10.1007/S11263-021-01555-8](https://doi.org/10.1007/S11263-021-01555-8) (2022).
17. Berry, R. B. *et al.* *The AASM Manual for the Scoring of Sleep and Associated Events: Rules, Terminology and Technical Specifications, Version 2.6* (American Academy of Sleep Medicine, Darien, Illinois, 2020).
18. Motamedi-Fakhr, S., Moshrefi-Torbati, M., Hill, M., Hill, C. M. & White, P. R. Signal processing techniques applied to human sleep EEG signals - A review. *Biomed. Signal Process. Control.* **10**, 21–33, DOI: [10.1016/J.BSPC.2013.12.003](https://doi.org/10.1016/J.BSPC.2013.12.003) (2014).
19. Grieger, N. Source code of the model presented in Grieger *et al.*, “Data-efficient sleep staging with synthetic time series pretraining”. <https://github.com/dslaborg/frequency-pretraining> (2024).
20. Guillot, A., Sauvet, F., Doring, E. H. & Thorey, V. DREAM open datasets: Multi-scored sleep datasets to compare human and automated sleep staging. *IEEE T. Neur. Sys. Reh.* **28**, 1955–1965, DOI: [10.1109/tnsre.2020.3011181](https://doi.org/10.1109/tnsre.2020.3011181) (2020).

21. Supratak, A. & Guo, Y. TinySleepNet: An efficient deep learning model for sleep stage scoring based on raw single-channel EEG. In *42nd Annual Int. Conf. of the IEEE Engineering in Medicine & Biology Society, EMBC 2020*, 641–644, DOI: [10.1109/EMBC44109.2020.9176741](https://doi.org/10.1109/EMBC44109.2020.9176741) (IEEE, Montreal, QC, Canada, 2020).
22. Hochreiter, S. & Schmidhuber, J. Long short-term memory. *Neural Comput.* **9**, 1735–1780, DOI: [10.1162/neco.1997.9.8.1735](https://doi.org/10.1162/neco.1997.9.8.1735) (1997).
23. Kingma, D. P. & Ba, J. Adam: A method for stochastic optimization. In Bengio, Y. & LeCun, Y. (eds.) *3rd Int. Conf. Learning Representations, ICLR*, DOI: [10.48550/arxiv.1412.6980](https://doi.org/10.48550/arxiv.1412.6980) (San Diego, CA, USA, 2015).
24. Sokolova, M. & Lapalme, G. A systematic analysis of performance measures for classification tasks. *Inf. Process. Manag.* **45**, 427–437, DOI: [10.1016/J.IPM.2009.03.002](https://doi.org/10.1016/J.IPM.2009.03.002) (2009).
25. Tharwat, A. Classification assessment methods. *Appl. Comput. Inform.* DOI: [10.1016/j.aci.2018.08.003](https://doi.org/10.1016/j.aci.2018.08.003) (2018).
26. He, K., Zhang, X., Ren, S. & Sun, J. Delving deep into rectifiers: Surpassing human-level performance on ImageNet classification. In *2015 IEEE Int. Conf. on Computer Vision, ICCV 2015*, 1026–1034, DOI: [10.1109/ICCV.2015.123](https://doi.org/10.1109/ICCV.2015.123) (IEEE Computer Society, Santiago, Chile, 2015).
27. Eldele, E. *et al.* Self-supervised learning for label-efficient sleep stage classification: A comprehensive evaluation. *IEEE T. Neur. Sys. Reh.* **31**, 1333–1342, DOI: [10.1109/tnsre.2023.3245285](https://doi.org/10.1109/tnsre.2023.3245285) (2023).
28. Alvarez-Estevéz, D. Challenges of applying automated polysomnography scoring at scale. *Sleep Med. Clin.* **18**, 277–292, DOI: [10.1016/j.jsmc.2023.05.002](https://doi.org/10.1016/j.jsmc.2023.05.002) (2023).
29. Fiorillo, L. *et al.* U-Sleep’s resilience to AASM guidelines. *npj Digit. Medicine* **6**, DOI: [10.1038/S41746-023-00784-0](https://doi.org/10.1038/S41746-023-00784-0) (2023).
30. Gaiduk, M., Serrano Alarcón, A., Seepold, R. & Martínez Madrid, N. Current status and prospects of automatic sleep stages scoring: Review. *Biomed. Eng. Lett.* **13**, 247–272, DOI: [10.1007/s13534-023-00299-3](https://doi.org/10.1007/s13534-023-00299-3) (2023).
31. Vallat, R. & Walker, M. P. An open-source, high-performance tool for automated sleep staging. *eLife* **10**, DOI: [10.7554/elife.70092](https://doi.org/10.7554/elife.70092) (2021).
32. Donckt, M. J. V. D. *et al.* Do not sleep on traditional machine learning: Simple and interpretable techniques are competitive to deep learning for sleep scoring. *Biomed. Signal Process. Control.* **81**, 104429, DOI: [10.1016/J.BSPC.2022.104429](https://doi.org/10.1016/J.BSPC.2022.104429) (2023).
33. Vaswani, A. *et al.* Attention is all you need. In Guyon, I. *et al.* (eds.) *Annu. Conf. Neural Information Processing Systems, NeurIPS*, 5998–6008 (Long Beach, CA, USA, 2017).
34. Brandmayr, G. *et al.* Relational local electroencephalography representations for sleep scoring. *Neural Networks* **154**, 310–322, DOI: [10.1016/J.NEUNET.2022.07.020](https://doi.org/10.1016/J.NEUNET.2022.07.020) (2022).
35. Dosovitskiy, A. *et al.* An image is worth 16x16 words: Transformers for image recognition at scale. In *Int. Conf. on Learning Representations, ICLR* (2021).
36. Zhang, G.-Q. *et al.* The national sleep research resource: Towards a sleep data commons. *J. Am. Med. Inform. Assn.* **25**, 1351–1358, DOI: [10.1093/jamia/ocy064](https://doi.org/10.1093/jamia/ocy064) (2018).
37. Obeid, I. & Picone, J. The Temple University hospital EEG data corpus. *Front. Neurosci.* **10**, DOI: [10.3389/fnins.2016.00196](https://doi.org/10.3389/fnins.2016.00196) (2016).

Acknowledgments

We are grateful to M. Reißel and V. Sander for providing us with computing resources.

Author contributions statement

N.G. and S.B. conceived the experiments; N.G. conducted the experiments; N.G., S.M., and S.B. analyzed and discussed the results; N.G. and S.B. wrote the first draft of the manuscript; N.G., S.M., and S.B. reviewed the manuscript.

Competing interests

The authors declare no competing interests.

Additional information

Correspondence and requests for materials should be addressed to S.B.